F. Bisconti, B. Vilardo, G. Corallo, F. Scalera, G. Gigli, A. Chiocchetti, A. Polini,* F. Gervaso*

An Assist for Arthritis Studies: A 3D Cell Culture of Human Fibroblast-Like Synoviocytes by Encapsulation in a Chitosan-Based Hydrogel

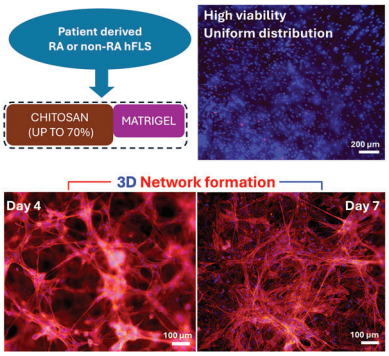

A chitosan-based hydrogel formulation is developed for 3D culturing of human fibroblast-like synoviocytes, derived from non-RA and RA patients. The hydrogel, consisting of 70% chitosan and 30% Matrigel, demonstrates superior stability and cell growth. This cost-effective system offers a viable alternative to sole Matrigel for synoviocytes encapsulation.

ADVANCED THERAPEUTICS
www.advtherap.com

An Assist for Arthritis Studies: A 3D Cell Culture of Human Fibroblast-Like Synoviocytes by Encapsulation in a Chitosan-Based Hydrogel

Francesco Bisconti, Beatrice Vilardo, Gaia Corallo, Francesca Scalera, Giuseppe Gigli, Annalisa Chiocchetti, Alessandro Polini, and Francesca Gervaso**

Osteoarthritis (OA) and Rheumatoid arthritis (RA) are the most common arthritis in which the synovium is involved, but the cellular and molecular basis of these pathologies still need better elucidation. Fibroblast-like synoviocytes (FLS), one of the cellular elements of the synovium, play a key role in RA, an autoimmune disease characterized by joint inflammation and systemic symptoms that afflicts 1% of worldwide population. Despite articular damage starts from synovium and then proceeds involving cartilage till bone erosion, several 3D in vitro models are reported for cartilage and bone while only a few studies focused on the synovial component. Here, a hydrogel formulation suitable for 3D culturing human fibroblast-like synoviocytes and evaluated its suitability with non-RA and RA patients derived-cells is developed. Among different formulations, a chitosan (Cs)-based hydrogel, constituted by 70% of Cs and 30% of Matrigel, showed the best results in terms of stability as well as cell growth and morphology: non-RA and RA FLS are able to grow within the hydrogel forming a complex 3D network. Thanks to the low cost, and high market availability of chitosan, this system represents a good alternative to the use of sole Matrigel for encapsulating human synoviocytes.

1. Introduction

Among the diverse forms of arthritis, Osteoarthritis (OA) and Rheumatoid Arthritis (RA) are the most common. OA afflicts every year 7% of the global population.[1] Also RA, an autoimmune form of arthritis, represents a systemic pathology that afflicts 1% of the world population, both women and men with a ratio ranging from 4:1 to 2:1 in the younger to older population. Articular joint pathologies are characterized by an interplay between the different articular tissues, mainly bone, cartilage, synovium. In both OA and RA, synovium is involved but has a predominantly role in RA. Rheumatoid arthritis is mostly spread in developed countries and it is a consequence of a complex interaction between genetic and environmental factors.[2] Besides systemic symptoms such as fatigue and weakness, the first reported symptomatology regards pain and swelling of the diarthrodial joints.

F. Bisconti, G. Corallo, F. Scalera, G. Gigli, A. Polini, F. Gervaso
CNR NANOTEC – Institute of Nanotechnology
c/o Campus Ecotekne
Via Monteroni, Lecce 73100, Italy
E-mail: alessandro.polini@nanotec.cnr.it;
francesca.gervaso@nanotec.cnr.it

B. Vilardo, A. Chiocchetti
Dipartimento di Scienze della Salute
Interdisciplinary Research Center of Autoimmune Diseases-IRCAD
Università del Piemonte Orientale
Novara 28100, Italy

B. Vilardo, A. Chiocchetti
Center for Translational Research on Autoimmune and Allergic Diseases
University of Piemonte Orientale
Novara 28100, Italy

G. Corallo
Dipartimento di Matematica e Fisica E. de Giorgi
Università del Salento
Campus Ecotekne
Via Monteroni, Lecce 73100, Italy

G. Gigli
Dipartimento di Medicina Sperimentale
Università del Salento
Campus Ecotekne
Via Monteroni, Lecce 73100, Italy

The ORCID identification number(s) for the author(s) of this article can be found under https://doi.org/10.1002/adtp.202400166

DOI: 10.1002/adtp.202400166

The inflammation process stems from synovium with the invasion of inflammatory macrophages, followed by the simultaneous activation of synovial tissue-resident macrophages (STM) and fibroblast-like synoviocytes (FLS).[3–7] Studies based on mass cytometry and single-cell RNA sequencing identified different subset populations of STM and FLS highlighting their role as potential target in RA. Under RA conditions, FLS acquire a more aggressive phenotype characterized by higher activation, proliferation, and invasion[8–10] Activated FLS lead to both cartilage degradation, due to the production of matrix metalloproteinases (MMPs), and bone erosion, by expression of receptor activator of NF-kB ligand which increases osteoclastogenesis.[11–13] Despite the importance of the synovial tissue in RA development and progression, in literature there is a conspicuous number of works related to the 3D in vitro culturing of the osteochondral component, but only a few reports focused on the synovium.[14–18] Thus, to recapitulate a 3D microenvironment, which is crucial to better mimic the in vivo condition,[19] FLS can be encapsulated in 3D matrices like hydrogels. Nevertheless, contrarily to different cell lines, only a limited number of data is available. Hydrogels suitable for the FLS culturing are GelMA[20] and Matrigel,[21,22] employed to produce cell-laden hydrogel drops seeded in Multiwell plates or integrated in organ-on-a-chip systems.[23,24] In addition to the limited choice of materials for FLS encapsulation, should be considered the properties of the most used Matrigel. It is an expensive, commercially available product derived from Engelbreth–Holm–Swarm mouse tumor, essentially constituted of laminin, collagen IV, entactin, and various growth factors (among them, fibroblast growth factor, epidermal growth factor, insulin-like growth factor 1, transforming growth factor beta, platelet- derived growth factor, and nerve growth factor). Behind these main components, analysis by liquid chromatography-mass spectroscopy identified over one thousand different proteins, some of them involved in metabolic pathways and other important biological processes, and highlighted also a lot-to-lot variation.[25] Taking into account Matrigel composition, many doubts arise on its influence on cell culture.[26–28] Therefore, with the aim to replace, or partially reduce, the amount of Matrigel for cell culture of hFLS, we developed hydrogel formulations based on a thermo-responsive chitosan(Cs)-based hydrogel. Cs is a linear polysaccharide with a random arrangement of β-(1–4)-linked d-glucosamine and N-acetyl-d-glucosamine, featured by intriguing properties like biodegradability, biocompatibility, low immunogenicity, and low cost. For this reason, its use for mammalian cells encapsulation is well-reported.[29–35] Hence, we developed a chitosan:Matrigel (Cs:Matrigel) hydrogel combining the two materials. The new formulations were first tested and validated encapsulating non-RA patients derived-hFLS, then employing RA hFLS. In both the cases, these systems allowed high cell viability and the formation of a complex 3D network, demonstrating to represent a cheaper and reliable alternative for reproducing a 3D in vitro synovial microenvironment.

2. Experimental Section

2.1. Hydrogel Preparation and Gelation

Matrigel hESC-Qualified Matrix, LDEV-free (#354 277, Corning, New York, US) was thawed in ice overnight and used without any dilution. Matrigel was incubated at 37 °C (5% CO_2) for 45 min to obtain complete gelation. To obtain Cs:Matrigel hydrogels, first a high content (3.33% w/v) solution of Cs (degree of deacetylation 75–85%, MW 50.000–190.000 Da, #448 869, Sigma Aldrich, Milan, Italy) was prepared in 0.1 M HCl. For the solubilization, Cs was gradually added to HCl, mixed with a spatula, and left under stirring overnight at 25 °C. The solution was centrifugated (2500 rpm for 10 min) to remove air bubbles and stored at 4 °C until further use. To obtain the thermo-responsiveness of Cs, a 0.5 M solution of β-glycerophosphate (disodium salt pentahydrate, MW 306.11 g mol^{-1}, #35 675, Sigma Aldrich) acted as a gelling agent (GA). Cs and GA solutions were manually mixed in a 3:2 ratio and incubated at 37 °C (5% CO_2) for 10 min to obtain the sol–gel transition. Then, Cs:Matrigel hydrogel was developed by the gentle mixing of Cs solution and Matrigel. 50:50 and 70:30 Cs:Matrigel (hereinafter referred as 50% Cs and 70% Cs, respectively) hydrogel formulations were optimized. For the first one, based on an equal volume concentration of high-content Cs solution and Matrigel, an incubation time of 20 min was used to obtain the gelation, while for the formulation based on 70% of Cs 15 min was employed.

2.2. Scanning Electron Microscopy (SEM)

A SEM investigation was conducted to analyze the ultrastructure of the hydrogels. The samples were freeze–dried and cut to obtain a transversal section. For the visualization by SEM EVO 40 (Carl Zeiss AG, Oberkochen, Germany), samples were previously coated with 10 nm layer of gold (CCU-010 HV, Safematic GmbH, Zizers, Switzerland). Image acquisition was carried out at different magnifications using an accelerating voltage of 10 kV.

2.3. Compression Test

To assess the mechanical properties of the hydrogels, a compression test was performed using a ZwickiLine 1 kN testing machine (Zwick Roell, Kennesaw, GA, USA), employing a 10 N load cell. The hydrogels were tested 2 h after the gelation (kept in wet condition by immersion in PBS). Three samples, about 3 mm high and with a diameter of 8 mm, for each hydrogel formulation were prepared and tested in compression. The test was conducted up to 75% deformation and with a displacement velocity of 2 mm min^{-1}. To evaluate the hydrogel stiffness in compression, Young's modulus was calculated for each sample as the slope of the initial linear part of the stress–strain curve (0-5%).

2.4. Cell Culture and Cell Encapsulation

Non-RA and RA patient-derived human fibroblast-like synoviocytes were isolated from arthroscopy surgery-derived biopsy and used after approval of the UPO ethical committee [OCEANIA CE/21]. Each biopsy was frozen prior to use. Thawing of biopsies of the synovial tissue was performed in a 6-well plate filled with 1 mL of pre-warmed Roswell Park Memorial Institute medium (RPMI) (Gibco, USA) with the addition of 5% of Fetal Bovine Serum (FBS) (Gibco, USA), (2 wells) and RPMI only (1 well) for

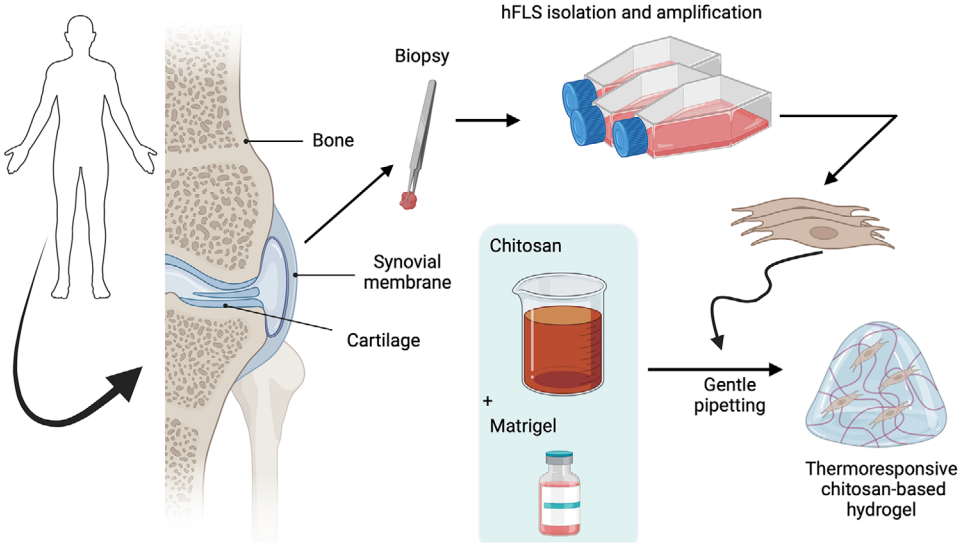

Figure 1. Original schematic representation of the process, from biopsy to cell encapsulation. Non-RA and RA patients-derived human fibroblast-like synoviocytes were isolated, amplified, then encapsulated in the hydrogel formulations previously prepared. Created with BioRender.com.

each sample. The frozen tissue sample in cryotubes was quickly emerged in a water bath at 37 °C with gentle swirling of the tube until complete melting of the ice. The samples were transferred into the well containing only RPMI and subsequently to the well containing pre-warmed 5%FBS/RPMI and incubated for 10 min at room temperature (RT) to wash out residues of the freezing media in the tissue. The samples were mixed gently several times during the incubation. After 10 min, the tissue samples were transferred to a second well-containing 5%FBS/RPMI and incubated for 40 min. After the incubation, the tissue samples were relocated to a well containing pre-warmed RPMI without serum to rinse the tissue. After thawing, the samples were cut-out into 2 × 2 mm pieces and immersed into digestion buffer (1 mg mL^{-1} collagenase type I in Dulbecco's modified Eagle's medium, DMEM/F12) (Gibco, USA) w/o FBS. Digestion was performed at 37 °C for 30 min. By adding 5 mL 10% FBS/DMEM/F12 the digestion process was stopped. After the digestion process, in order to attach the pieces to the flask (T75), the pieces were left in the flask without medium for 20 min in the incubator. After incubation of 20 min, the medium (10% FBS/DMEM/F12) with extracted cells was added. The flasks with the pieces were left in the incubator until the majority of the cells left the extracellular matrix. The cells were left in the flask to proliferate with the medium changing every 2/3 days. Subsequently, some days after (5–10 days), the pieces that were left in the flask were discarded. After this procedure, hFLS were used till passage 5 using DMEM supplemented with 2 mM glutamine, 10% FBS, 100 U mL^{-1} penicillin, and 100 g mL^{-1} streptomycin (Gibco, USA). Cells were incubated at 37 °C, 5% CO_2 and the medium was changed every 3 days until a cell confluence of 50%, then each other day. For hydrogel encapsulation, hFLS were embedded at a concentration of 2 M mL^{-1} of hydrogel. All the hydrogel formulations (Matrigel, 50% Cs, 70% Cs, Cs) were kept in ice before the encapsulation. Importantly, once the cells were detached by trypsin (Corning), they were resuspended in DMEM and embedded in the hydrogel solution in a 1:5 ratio (cell suspension: hydrogel) followed by gentle pipetting. Then, drops of 30 µL of cell laden hydrogel were dispensed on a 24-well tissue culture-treated plate (Corning), following the optimized time of incubation for each hydrogel. After that, 500 µL of DMEM was added into each well, changing medium each other day. A schematic representation of the process is reported in **Figure 1**.

2.5. Viability Assay

Live and dead assay at day 1 was conducted to evaluate the cell viability of encapsulated hFLS. For non-RA patient-derived hFLS a blue/red cell viability imaging kit (ReadyProbes, Invitrogen, Milan, Italy) was used following the protocol suggested by the manufacturer. Briefly, the working solution was prepared by adding two drops (kit dispenser dosed) of NucBlue Live reagent and two drops of propidium iodide (PI) to each mL of culture medium. Whilst, in the case of RA hFLS, a calcein AM-PI iodine staining, based on a 50 µg mL^{-1} PI solution supplemented with 1% of 2 mM calcein AM, was used. In both the protocols, DMEM was removed from the samples, following a washing step with PBS and the addition of the working solutions. Samples were incubated at 37 °C for 2 h in the dark. At the end of the incubation time, the samples were washed with PBS and the images were acquired by fluorescence microscopy (Axio Zoom.V16, Zeiss, Oberkochen, Germany) at the following wavelengths: 360 nm for NucBlue Live reagent (all cells), 535 nm for propidium iodide (dead cells), 488 nm for calcein-AM (live cells).

2.6. Cell Morphology Assessment

At day 4 and day 7 of cell encapsulation, a DAPI-Phalloidin staining was carried out to assess cell morphology inside the hydrogel formulations. The following protocol was used: samples were washed two times with PBS, fixed in 4% PFA (Corning) in PBS for 10 min, rinsed two times with PBS, permeabilized with 0.2% Triton X-100 in PBS, rinsed two times with PBS, blocked

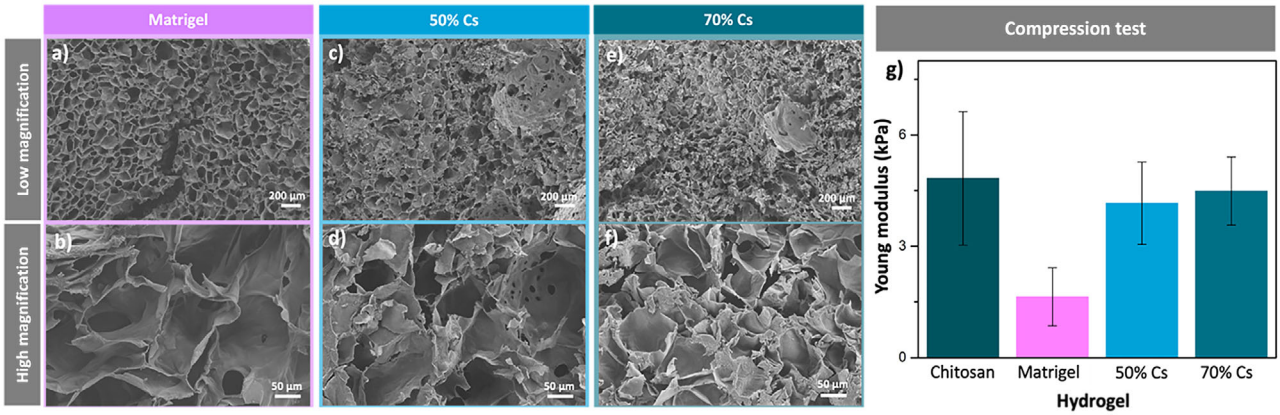

Figure 2. Hydrogel characterization. SEM images acquired at low and high magnification of a,b) Matrigel, c,d) 50% Cs, e,f) 70% Cs. In g), the results of the compression test. Although the samples had a similar morphology, the compression test highlighted the influence of chitosan on the mechanical properties of the different formulations.

with 5% BSA in PBS for 45 min. Actin filaments were stained with Phalloidin–tetramethylrhodamine B isothiocyanate (Sigma-Aldrich) diluted 1:500 in PBS (25 min), while nuclei were stained with DAPI (Sigma–Aldrich) diluted 1:10 000 in PBS (20 min). The samples were washed two times with PBS and analyzed by fluorescence microscopy (EVOS M7000, Thermo-Fisher, Milan, Italy).

3. Results

3.1. Hydrogel Ultrastructure and Mechanical Properties

Transversal sections of the hydrogels were prepared and analyzed by SEM. 50% Cs and 70% Cs hydrogel formulations exhibited structure and apparent porosity similar to those of sole Matrigel (**Figure** 2a–f), showing therefore no evident impact strictly connected to the ratio of the two components. Differently, the mechanical properties were strongly affected by the Cs:Matrigel ratio (Figure 2g), as expected. While Matrigel displayed a Young's modulus of 1.6 kPA, this was increased almost three-fold for 50% Cs and 70% Cs (4.1 and 4.5 kPa, respectively), approaching the value of the sole Cs (4.8 kPa).

3.2. Cell Viability of Non-RA Patient Derived-hFLS

Live and dead assay was performed to assess non-RA patient derived-hFLS viability in the developed hydrogel formulations. The results are reported in **Figure** 3, depicting the outer regions (upper row) and inner regions (bottom row) of the hydrogel drops. The different nature of Cs and Matrigel did not impact the cell distribution inside the hydrogel, which appeared highly homogeneous in all the conditions. Importantly, cell viability at day 1 for 50:50 and 70:30 Cs: Matrigel was comparable to that of Matrigel, showing no differences between the outer area of the hydrogel and the core of the drop.

3.3. Cell Morphology of Non-RA Patient Derived-hFLS

We assessed non-RA patient derived-hFLS elongation by carrying out a DAPI-Phalloidin staining at day 4 and day 7. hFLS acquired a typical fibroblast morphology after 4 days from cell encapsulation, as observable from **Figure** 4. This result was noticeable in all the hydrogel formulations. Particularly, in the case of 50% Cs we witnessed the formation of a complex 3D network of hFLS extended throughout the matrix, similarly to Matrigel.

Thus, we repeated a DAPI-Phalloidin staining after 7 days of 3D culture (**Figure** 5). Remarkably, hFLS resulted in a denser network as result of good cell proliferation and cell–cell interaction. Furthermore, also 70% Cs provided a suitable 3D architecture, similarly to 50% Cs and Matrigel.

3.4. Cell Viability and Cell Morphology of RA Patient-Derived hFLS

Live/dead assay and DAPI-Phalloidin staining were carried out on encapsulated RA hFLS, the results are reported in **Figure** 6. At day 1, similar results among the different hydrogel formulations, comparable to those obtained with non-RA hFLS, were obtained. Indeed, we recorded high cell viability and a uniform cell distribution across the entire hydrogel structure. Then, DAPI-Phalloidin staining was conducted to assess cell morphology at day 4 and day 7. After 4 days, RA hFLS started to elongate in Matrigel, 50% Cs, and 70% Cs hydrogels, while in the sole chitosan cells retained a rounded shape. Besides the cell elongation, we noted that after 3 days Matrigel drops underwent a degradation process, leading to an almost complete degradation of the drop after 7 days. DAPI-Phalloidin at day 7 allowed to observe the formation of a 3D hFLS network not only in Matrigel samples, but also in the formulations based on 50 and 70% of Cs. Clearly, in the case of the sole Matrigel, it must be taken into account that the images were acquired on hydrogel fragments consisting of a few millimeters of structure.

4. Discussion

Rheumatoid arthritis is an autoimmune disease for which in the last years few 3D in vitro models have been developed.[36] In recent years, various systems have been presented for bone and

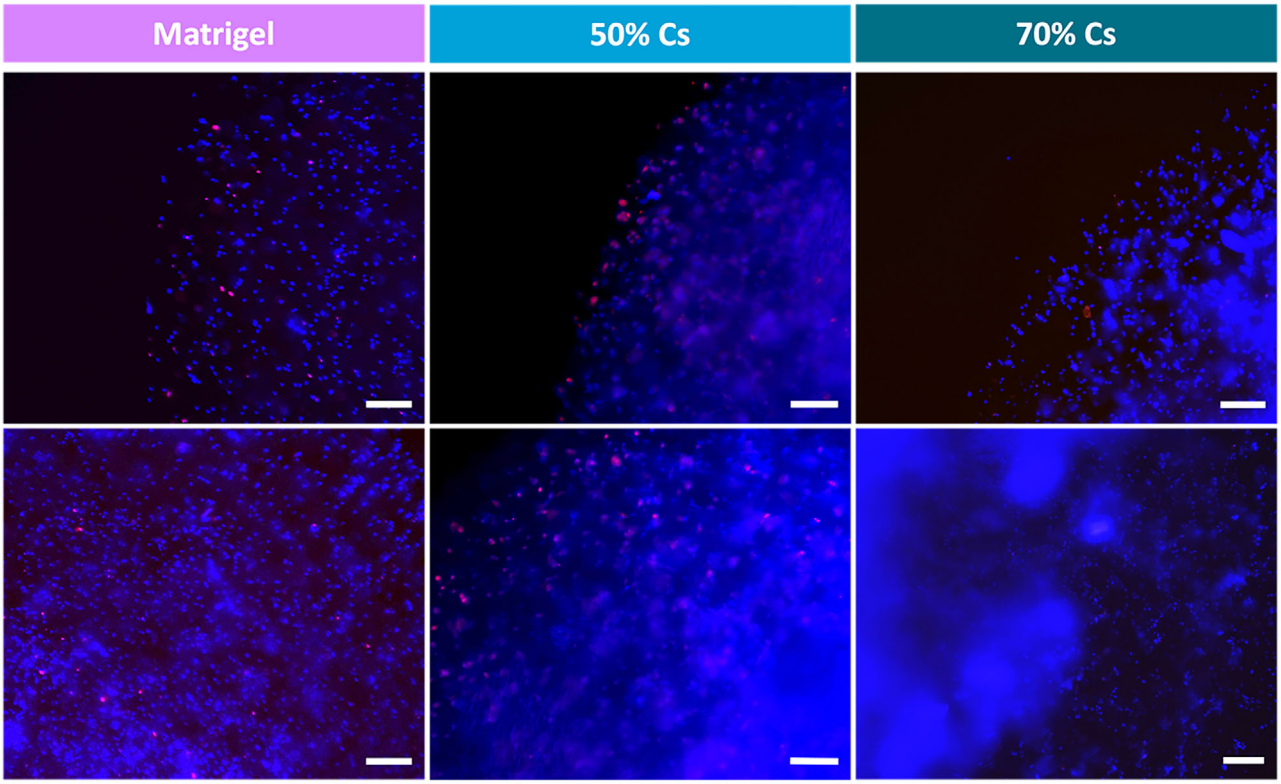

Figure 3. Non-RA hFLS viability in the hydrogel formulations at day 1. Outer regions (upper row) and inner regions (bottom row) of the hydrogel drops were imaged. Blue signal refers to the nuclei of all cells, and red to the nuclei of the dead cells. High cell viability was recorded in all the formulations, with no evident variation regarding the drop structure. Scale bar: 200 µm.

cartilage, but just a few models were focused on the synovium.[24] This hampers the modeling of a more complex joint in vitro that should consider the intricate crosstalk that takes place between the synovium and the other tissues (cartilage, bone, and the vascular system). Cell–cell communication within the tissues of the joint is complex and still not completely clear,[13,37–39] highlighting the need for reliable cellular models.

Considering the synovium tissue, constituted by human fibroblast-like synoviocytes and tissue-resident macrophages, most of the studies reported in literature regard the 3D in vitro culturing of human fibroblast-like synoviocytes, employing Matrigel as matrix. Kiener et al., and later Broener et al., used Matrigel for the encapsulation of hFLS producing a 3D in vitro model and observing the formation of a lining at the interface between the hydrogel and culture medium.[21,40] More recently, Peter Ertl group evaluated different matrices for hFLS encapsulation comparing Matrigel with PEG-dextran and Tisseel fibrin hydrogels prior the integration on a chip platform.[23] In that study, one of the hydrogel formulations was discarded because its turbidity was not compatible with the 3D biosensing acquisition system, highlighting the importance of the hydrogel properties in a broad spectrum of requirements. Few alternative hydrogels are reported in literature for the FLS culturing, like GelMA that was used for synoviocytes bioprinting.[20] Thus, Matrigel is the most used and eligible material, but it is also characterized by several disadvantages like poor availability, high cost, lot-to-lot variation, and has a debated influence on cell culture due to the presence of several growth factors.[25,27] Toward a reduction in the use of such material for in vitro models, herein, we developed a hydrogel formulation combining the well-known Matrigel with the more affordable and characterized chitosan.

Resultant 50% Cs and 70% Cs hydrogels retained a thermoresponsive behavior with a sol–gel transition at 37 °C after 20 and 15 min, respectively, therefore quicker than the sole Matrigel which required a longer time of gelation, 45 min, as also reported elsewhere.[21,22,40] We primarily analyzed the hydrogel microarchitecture by SEM. Matrigel and Cs-based formulations displayed an interconnected architecture similar to those reported in literature for these materials.[41,42] The surface at the micrometer scale resulted quite similar in terms of apparent porosity and pore size among all the samples. On the contrary, the influence of chitosan concentration was evident on the mechanical properties of the hydrogel formulations. We analyzed the hydrogel stiffness under compression and calculated the Young's modulus as the slope of the linear part of the stress–strain curve. Matrigel matrix showed a modulus of 1.6 kPa, while the hydrogel based on 70% of Cs revealed a modulus of 4.5 kPa, close to that of Cs (4.8 kPa). Beyond this slight difference, the recorded values are within a range compatible with human tissues where human fibroblasts are present, as elegantly reviewed by Guimarães et. al.[43]

To evaluate the suitability of these hydrogels for the encapsulation of human fibroblast-like synoviocytes, we first encapsulated non-RA hFLS, carrying out a Live and dead assay at day 1, followed by a DAPI-Phalloidin staining at day 4 and day 7 aimed

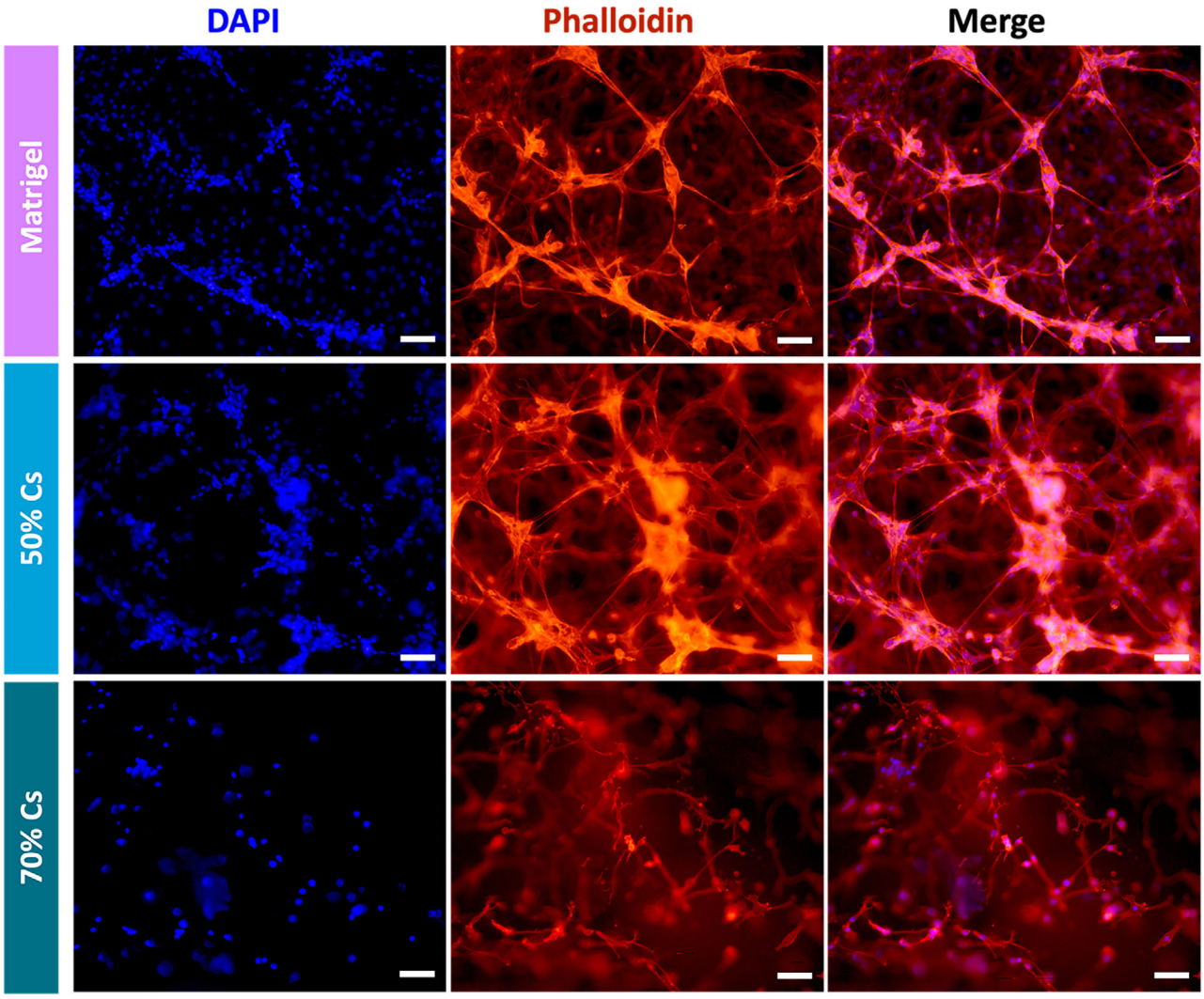

Figure 4. DAPI-Phalloidin staining at day 4. Nuclei in blue, actin filaments in red in non-RA hFLS. A 50% Cs formulation ensured a 3D network of hFLS similar to the one displayed by pure Matrigel. Scale bar: 100 µm.

at assessing hFLS elongation. Live and dead assay allowed us to observe that we could obtain an ideal cell distribution along the entire hydrogel structure and, importantly, cell viability of 50% Cs and 70% Cs formulations was equivalent to that of Matrigel. However, as often reported in biopolymer-derived hydrogels a slight increase in the blue fluorescence signal, appearing as cloud-like formations, is attributed to the presence of chitosan in the hydrogel formulations.[44,45] hFLS appeared to acquire their typical fibroblast-like morphology just after 4 days from cell encapsulation in all the hydrogel formulations and established a complex 3D network. Despite the high content of chitosan, we were able to perform fluorescence imaging and obtained good-quality images. This feature is of crucial importance for a proper imaging-based characterization. For example, Rothbauer et al. carried out a preliminary analysis on diverse hydrogels for hFLS encapsulation and discarded one of these due to poor compatibility with their imaging system.[23] At day 7, 50% Cs and, importantly, 70% Cs, revealed a denser network of hFLS as a demonstration of the validity of the hydrogels. Contrarily to previous data reported in the literature, where a lining and sub-lining architecture were highlighted,[21,22] we obtained a marked cell elongation in the hydrogel structure, likely due to a better exchange of nutrients throughout the drop.

Comparable results in terms of cell viability and morphology were obtained by encapsulating hFLS derived from Rheumatoid arthritis patients. Hydrogels based on 50% and 70% of chitosan enabled high cell viability, like that of sole Matrigel, and allowed hFLS to elongate and finally form a 3D network after 7 days. Notably, huge differences among the different hydrogels emerged in terms of material stability. The hydrogel of sole Matrigel underwent to a degradation process just after 4 days, while the formulations based on chitosan retained the original structure till the end of the experiment. This finding is likely the results of the enzymatic activity of activated hFLS.[46] Indeed, under RA condition, synoviocytes are recognized to acquire an activated phenotype, characterized by tumor-like behavior and resulting in increasing production of matrix metalloproteinases (like MMP1, MMP13, MMP3). Importantly, this phenotype is retained in vitro.[47] Our

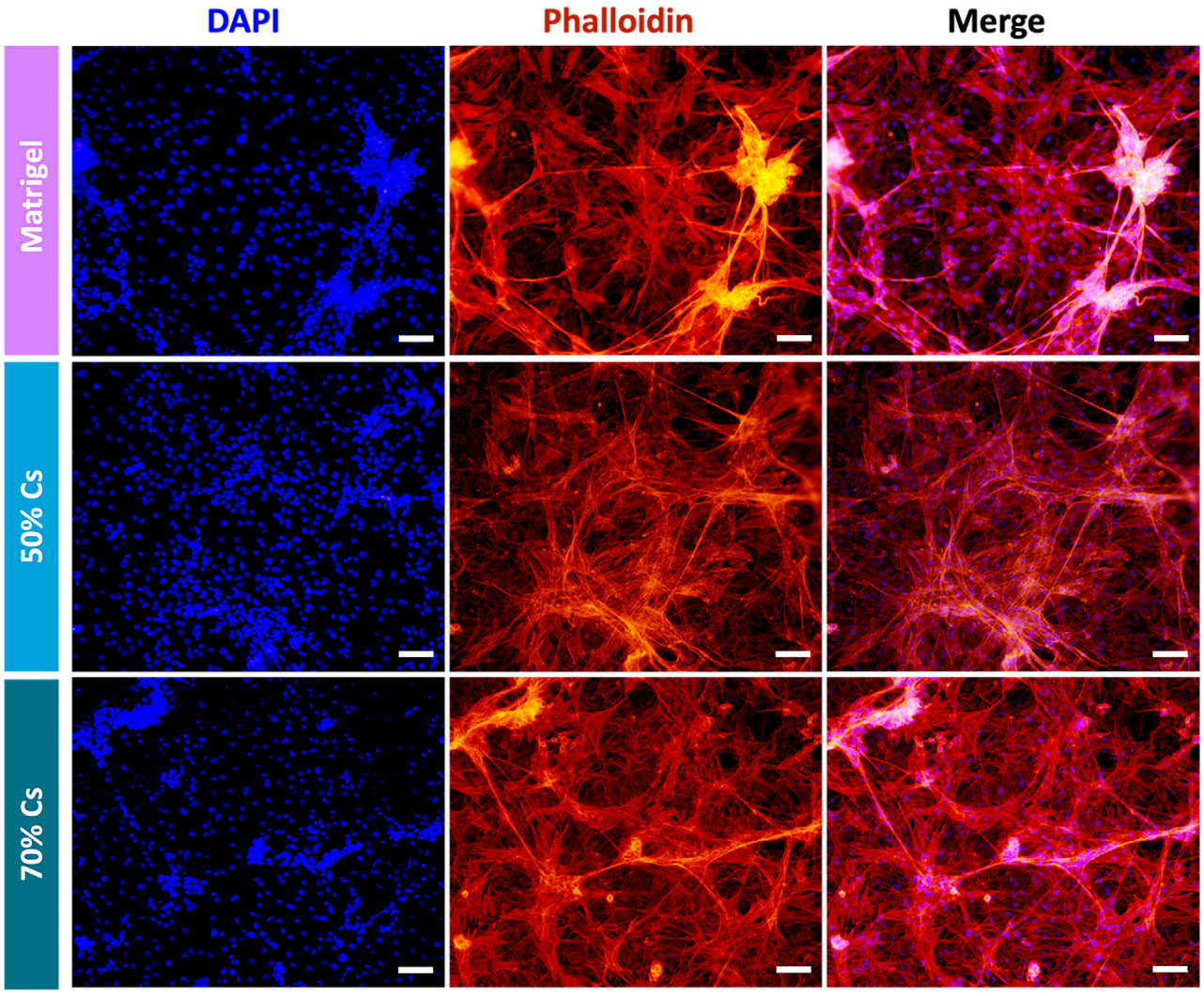

Figure 5. DAPI-Phalloidin staining at day 7. Nuclei in blue, actin filaments in red in non-RA hFLS. Both Cs-based formulations allowed the development of a dense 3D cellular network. Scale bar: 100 µm.

observation of the higher stability of chitosan-based formulations in the RA hFLS model can be explained by the nature of MMPs. MMPs are a family of proteolytic enzymes responsible for degrading various components of the extracellular matrix, including collagen, elastin, gelatin, and proteoglycans.[48,49] However, chitosan, a polysaccharide derived from chitin through deacetylation, is not a protein but a polysaccharide. MMPs specifically target protein substrates (which are abundant in Matrigel) and do not have activity against polysaccharides like chitosan. The degradation of chitosan requires specific enzymes such as chitosanase, which can cleave the glycosidic bonds in chitosan.[50,51] Since MMPs cannot digest chitosan, a higher concentration of chitosan probably ensured greater stability of the entire hydrogel. Thus, the degradation occurred at 4 days in the case of RA cell encapsulation underlines that the stability, in addition to other material characteristics like cytotoxicity, stiffness, and biocompatibility, is a crucial factor for the selection of a proper hydrogel for recapitulating a specific tissue. Hydrogel formulations must allow high cell viability, proliferation, and elongation, and a lifespan compatible with the experimental plan.[52] The data reported here show that chitosan-based hydrogels represent an eligible biomaterial for the 3D culturing of non-RA and RA patients derived-human fibroblast-like synoviocytes, an interesting result also considering the limited choice of hydrogels suitable for this cell population. Unlike traditional 2D cultures, this 3D model offers a more physiologically relevant environment for examining cellular behavior under inflammatory conditions or assessing drug effects. Future work will focus on further reducing or totally replacing Matrigel with more cost-effective, protein-rich matrices and optimizing the model. This approach aims to provide a versatile platform for the scientific community, enhancing the study of synovial inflammation and the development of novel therapeutic strategies. We believe this system holds great potential for advancing the understanding of synovial pathology and facilitating the translational research necessary for the development of effective treatments.

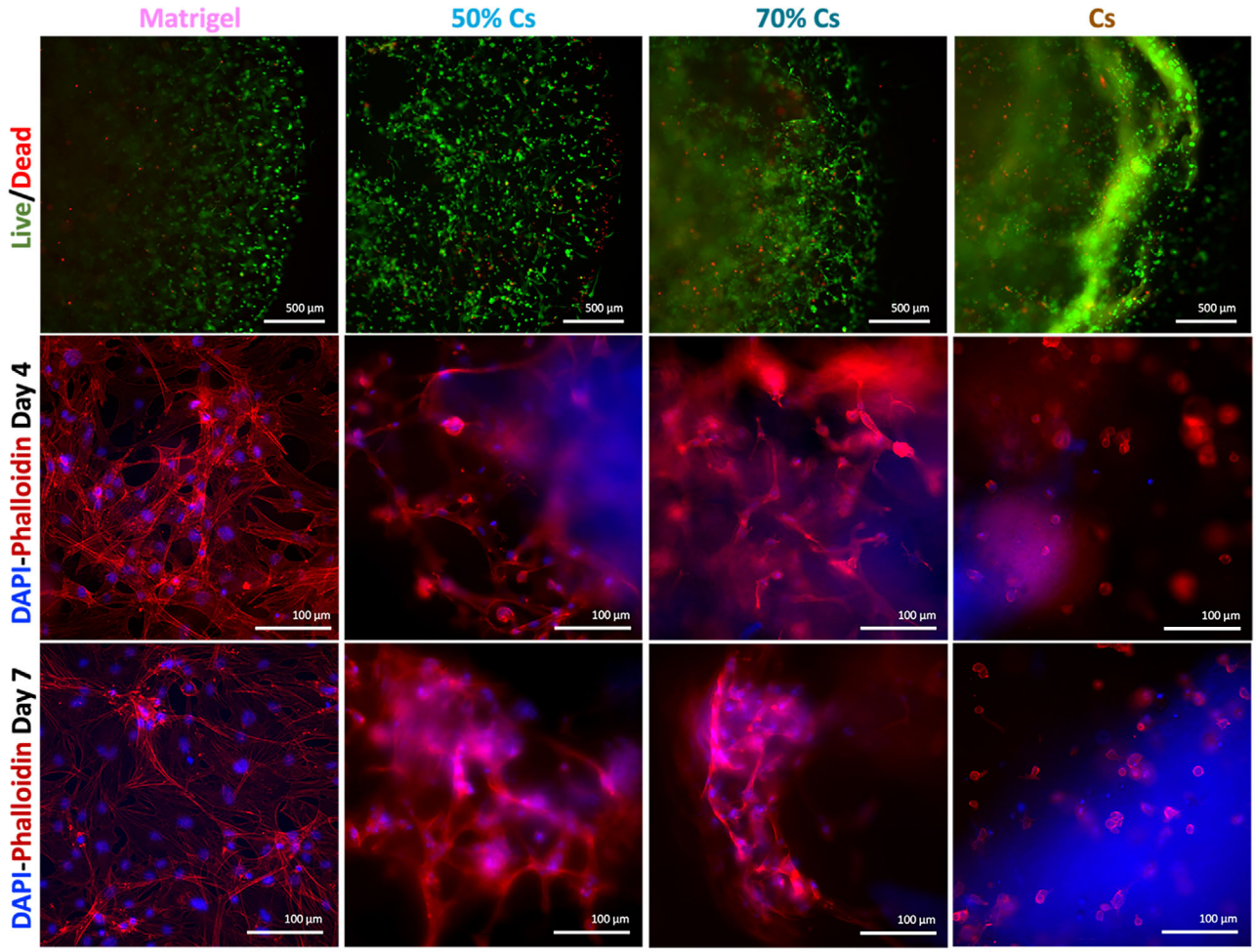

Figure 6. Cell viability and morphology of RA patient-derived hFLS. Live/dead assay at day 1 (live cells in green, dead cells in red) in the first row; DAPI-Phalloidin staining at day 4 and day 7 in the second and third rows, respectively. The viability and cell morphology results are similar to those obtained with non-RA hFLS.

5. Conclusion

Synovial tissue is involved in very common and widespread pathologies like Osteoarthritis and, particularly, Rheumatoid arthritis. The development of 3D in vitro culturing systems of human fibroblast-like synoviocytes, a key element of synovium, becomes therefore essential in this context. With the aim to replace, or partially reduce, the use of Matrigel, the most popular matrix employed in literature for hFLS, we tested the use of chitosan, a more affordable and available material. A hydrogel formulation based on 70% of chitosan resulted as a stable material that allowed high cell viability and the formation of a complex 3D network within the hydrogel that is comparable to the more popular Matrigel, as demonstrated by Live and dead assay and by DAPI-Phalloidin staining conducted on non-RA and RA hFLS. Thanks to a lower cost compared to the use of pure Matrigel, and high market availability, this system represents a good alternative to the most known and most used synoviocytes encapsulation in the sole Matrigel. While Matrigel remains necessary, reducing its amount by 70% represents a significant cost saving, an important factor crucial for enabling research in this field to be accessible to a broader range of researchers. Moreover, to the best of our knowledge, the 3D network of human hFLS in a Cs-based hydrogel has been reported for the first time.

Acknowledgements

The authors are grateful to the support from the European Union's Horizon 2020 research and innovation programme under grant agreement No. 953121 (FLAMIN-GO), the "Tecnopolo per la medicina di precisione" (TecnoMed Puglia) – Regione Puglia: DGR n.2117 del 21/11/2018, CUP: B84I18000540002, and from the Italian Ministry of Research (MUR) under the EU NRRP "National Center for Gene Therapy and Drugs based on RNA Technology" (Project no. CN00000041 CN3 RNA) and the complementary actions to the EU NRRP "FIT4MedRob" Grant (contract number CUP B53C22006960001) and "D34 Health" (contract number CUP B53C22006100001).

Open access publishing facilitated by Consiglio Nazionale delle Ricerche, as part of the Wiley - CRUI-CARE agreement.

Conflict of Interest

The authors declare no conflict of interest.

Author Contributions

F.B. performed methodology, investigation, formal analysis, data curation, wrote, reviewed & edited the first draft. B.V. did Investigation, wrote, reviewed & edited the final manuscript. G.C. did investigation. F.S. did Investigation. G.G. acquired resources. A.C. acquired resources, supervised the project, and performed discussion, wrote, reviewed & edited the final manuscript. A.P. acquired resources, performed conceptualization, investigation, supervised the project, and performed discussion, and wrote, reviewed & edited the final manuscript. F.G. acquired resources, performed conceptualization, investigation, Discussion, supervised the project, and performed discussion and wrote, reviewed & edited the final manuscript.

Data Availability Statement

The data that support the findings of this study are available from the corresponding author upon reasonable request.

Keywords

hydrogels, in vitro models, rheumatoid arthritis, synovium

Received: April 19, 2024
Revised: July 1, 2024
Published online:

[1] E. Sanchez-Lopez, R. Coras, A. Torres, N. E. Lane, M. Guma, *Nat. Rev. Rheumatol.* **2022**, *18*, 258.
[2] A. Finckh, B. Gilberti, B. Hodkinson, S. C. Bae, R. Thomas, K. D. Deane, D. Alpizar-Rodriguez, K. Lauper, *Nat. Rev. Rheumatol.* **2022**, *18*, 591.
[3] C. Orr, E. Vieira-Sousa, D. L. Boyle, M. H. Buch, C. D. Buckley, J. D. Cañete, A. I. Catrina, E. H. S. Choy, P. Emery, U. Fearon, A. Filer, D. Gerlag, F. Humby, J. D. Isaacs, S. A. Just, B. R. Lauwerys, B. Le Goff, A. Manzo, T. McGarry, I. B. McInnes, A. Najm, C. Pitzalis, A. Pratt, M. Smith, P. P. Tak, S. W. Tas, R. Thurlings, J. E. Fonseca, D. J. Veale, *Nat. Rev. Rheumatol.* **2017**, *13*, 463.
[4] S. Alivernini, L. MacDonald, A. Elmesmari, S. Finlay, B. Tolusso, M. R. Gigante, L. Petricca, C. Di Mario, L. Bui, S. Perniola, M. Attar, M. Gessi, A. L. Fedele, S. Chilaka, D. Somma, S. N. Sansom, A. Filer, C. McSharry, N. L. Millar, K. Kirschner, A. Nerviani, M. J. Lewis, C. Pitzalis, A. R. Clark, G. Ferraccioli, I. Udalova, C. D. Buckley, E. Gremese, I. B. McInnes, T. D. Otto, *Nat. Med.* **2020**, *26*, 1295.
[5] M. Kurowska-Stolarska, S. Alivernini, *Nat. Rev. Rheumatol.* **2022**, *18*, 384.
[6] S. Kemble, A. P. Croft, *Front. Immunol.* **2021**, *12*, 1.
[7] T. Griffin, A. Scanzello, O. A. Macrophages in, *Clin. Exp. Rheumatol.* **2019**, *37*, s57.
[8] F. Zhang, K. Wei, K. Slowikowski, C. Y. Fonseka, D. A. Rao, S. Kelly, S. M. Goodman, D. Tabechian, L. B. Hughes, K. Salomon-Escoto, G. F. M. Watts, A. H. Jonsson, J. Rangel-Moreno, N. Meednu, C. Rozo, W. Apruzzese, T. M. Eisenhaure, D. J. Lieb, D. L. Boyle, A. M. Mandelin, B. F. Boyce, E. DiCarlo, E. M. Gravallese, P. K. Gregersen, L. Moreland, G. S. Firestein, N. Hacohen, C. Nusbaum, J. A. Lederer, H. Perlman, *Nat. Immunol.* **2019**, *20*, 928.
[9] A. Filer, *Curr. Opin. Pharmacol.* **2013**, *13*, 413.
[10] R. I. Ainsworth, D. Hammaker, G. Nygaard, C. Ansalone, C. Machado, K. Zhang, L. Zheng, L. Carrillo, A. Wildberg, A. Kuhs, M. N. D. Svensson, D. L. Boyle, G. S. Firestein, W. Wang, *Nat. Commun.* **2022**, *13*, 6221.
[11] N. Komatsu, H. Takayanagi, *Nat. Rev. Rheumatol.* **2022**, *18*, 415.
[12] T. Wada, T. Nakashima, N. Hiroshi, J. M. Penninger, *Trends Mol. Med.* **2006**, *12*, 17.
[13] T. Pap, A. Korb-Pap, *Nat. Rev. Rheumatol.* **2015**, *11*, 606.
[14] L. Banh, K. K. Cheung, M. W. Y. Chan, E. W. K. Young, S. Viswanathan, *Osteoarthritis Cartilage* **2022**, *30*, 1050.
[15] E. Kahraman, R. Ribeiro, M. Lamghari, E. Neto, *Front. Immunol.* **2022**, *13*, 802440.
[16] P. Occhetta, A. Mainardi, E. Votta, Q. Vallmajo-Martin, M. Ehrbar, I. Martin, A. Barbero, M. Rasponi, *Nat. Biomed. Eng.* **2019**, *3*, 545.
[17] C. A. Paggi, L. M. Teixeira, S. Le Gac, M. Karperien, *Nat. Rev. Rheumatol.* **2022**, *18*, 217.
[18] C. A. Paggi, J. Hendriks, M. Karperien, S. Le Gac, *Lab Chip* **2022**, *22*, 1815.
[19] R. Xie, V. Pal, Y. Yu, X. Lu, M. Gao, S. Liang, M. Huang, W. Peng, I. T. Ozbolat, *Biomaterials* **2024**, *304*, 122408.
[20] M. Petretta, S. Villata, M. P. Scozzaro, L. Roseti, M. Favero, L. Napione, F. Frascella, C. F. Pirri, B. Grigolo, E. Olivotto, *Applied Sciences (Switzerland)* **2023**, *13*.
[21] H. P. Kiener, D. M. Lee, S. K. Agarwal, M. B Brenner, *Am. J. Pathol.* **2006**, *168*, 1486.
[22] H. P. Kiener, G. F. M. Watts, Y. Cui, J. Wright, T. S. Thornhill, M. Sköld, S. M. Behar, B. Niederreiter, J. Lu, M. Cernadas, A. J. Coyle, G. P. Sims, J. Smolen, M. L. Warman, M. B. Brenner, D. M. Lee, *Arthritis Rheum.* **2010**, *62*, 742.
[23] M. Rothbauer, G. Höll, C. Eilenberger, S. R. A. Kratz, B. Farooq, P. Schuller, I. Olmos Calvo, R. A. Byrne, B. Meyer, B. Niederreiter, S. Küpcü, F. Sevelda, J. Holinka, O. Hayden, S. F. Tedde, H. P. Kiener, P. Ertl, *Lab Chip* **2020**, *20*, 1461.
[24] M. Rothbauer, R. A. Byrne, S. Schobesberger, I. Olmos Calvo, A. Fischer, E. I. Reihs, S. Spitz, B. Bachmann, F. Sevelda, J. Holinka, W. Holnthoner, H. Redl, S. Toegel, R. Windhager, H. P. Kiener, P. Ertl, *Lab Chip* **2021**, *21*, 4128.
[25] C. S. Hughes, L. M. Postovit, G. A. Lajoie, *Proteomics* **2010**, *10*, 1886.
[26] E. Polykandriotis, A. Arkudas, R. E. Horch, U. Kneser, *Am. J. Pathol.* **2008**, *172*, 1441.
[27] M. T. Kozlowski, C. J. Crook, H. T. Ku, *Commun. Biol.* **2021**, *4*, 1387.
[28] M. Wang, H. Yu, T. Zhang, L. Cao, Y. Du, Y. Xie, J. Ji, J. Wu, *Mol. Cell. Prot.* **2022**, *21*, 100181.
[29] M. C. G. Pellá, M. K. Lima-Tenório, E. T. Tenório-Neto, M. R. Guilherme, E. C. Muniz, A. F. Rubira, *Carbohydr. Polym.* **2018**, *196*, 233.
[30] E. Assaad, M. Maire, S. Lerouge, *Carbohydr. Polym.* **2015**, *130*, 87.
[31] A. Stanzione, A. Polini, V. La Pesa, A. Quattrini, A. Romano, G. Gigli, L. Moroni, F. Gervaso, *Biomater. Sci.* **2021**, *9*, 7492.
[32] G. Morello, A. Quarta, A. Gaballo, L. Moroni, G. Gigli, A. Polini, F. Gervaso, *Carbohydr. Polym.* **2021**, *274*, 118633.
[33] G. Morello, G. De Iaco, G. Gigli, A. Polini, F. Gervaso, *Gels* **2023**, *9*, 132.
[34] A. Stanzione, A. Polini, V. La Pesa, A. Romano, A. Quattrini, G. Gigli, L. Moroni, F. Gervaso, *Applied Sciences (Switzerland)* **2020**, *10*.
[35] B. Canciani, F. Semeraro, V. R. Herrera Millar, F. Gervaso, A. Polini, A. Stanzione, G. M. Peretti, A. Di Giancamillo, L. Mangiavini, *Int. J. Mol. Sci.* **2023**, *24*, 10446.
[36] Z. A. Li, S. Sant, S. K. Cho, S. B. Goodman, B. A. Bunnell, R. S. Tuan, M. S. Gold, H. Lin, *Trends Biotechnol.* **2023**, *41*, 511.
[37] C.-H. Chou, V. Jain, J. Gibson, D. E. Attarian, C. A. Haraden, C. B. Yohn, R.-M. Laberge, S. Gregory, V. B. Kraus, *Sci. Rep.* **2020**, *10*, 10868.
[38] M. Wang, G. Tan, H. Jiang, A. Liu, R. Wu, J. Li, Z. Sun, Z. Lv, W. Sun, D. Shi, *Bone Joint Res.* **2022**, *11*, 862.
[39] K. N. Bailey, T. Alliston, *Curr. Rheumatol. Rep.* **2022**, *24*, 184.

[40] M. Broeren, C. E. J. Waterborg, R. Wiegertjes, R. M. Thurlings, M. I. Koenders, P. L. E. Van Lent, P. M. Van deer Kran, F. A. J. Van de Loo, *ALTEX* **2019**, *36*, 18.
[41] H. Qin, J. Wang, T. Wang, X. Gao, Q. Wan, X. Pei, *Front. Chem.* **2018**, *6*.
[42] H. J. Kim, D. X. Oh, S. Choy, H. L. Nguyen, H. J. Cha, D. S. Hwang, *Cellulose* **2018**, *25*, 7299.
[43] C. F. Guimarães, L. Gasperini, A. P. Marques, R. L. Reis, *Nat. Rev. Mater.* **2020**, *5*, 351.
[44] Y. J. Cheah, M. H. M. Yunus, M. B. Fauzi, Y. Tabata, Y. Hiraoka, S. J. Phang, M. R. Chia, M. R. Buyong, M. D. Yazid, *Cellulose* **2023**, *30*, 5071.
[45] A. Przekora, G. Ginalska, *Cent. Eur. J. Biol.* **2014**, *9*, 634.
[46] K. Klein, P. A. Kabala, A. M. Grabiec, R. E. Gay, C. Kolling, L.-L. Lin, S. Gay, P. P. Tak, R. K. Prinjha, C. Ospelt, K. A. Reedquist, *Ann. Rheum. Dis.* **2016**, *75*, 422.
[47] Bottini, G. S. Firestein, *Nat. Rev. Rheumatol.* **2013**, *9*, 24.
[48] L. G. N. de Almeida, H. Thode, Y. Eslambolchi, S. Chopra, D. Young, S. Gill, L. Devel, A. Dufour, *Pharmacol. Rev.* **2022**, *74*, 712.
[49] H. Laronha, J. Caldeira, *Cells* **2020**, *9*, 1076.
[50] S. V. Gohil, A. Padmanabhan, H. M. Kan, M. Khanal, L. S. Nair, *Tissue Eng. Part A* **2021**, *27*, 867.
[51] L. Hartl, S. Zach, V. Seidl-Seiboth, *Appl. Microbiol. Biotechnol.* **2012**, *93*, 533.
[52] S. R. Caliari, J. A. Burdick, *Nat. Methods* **2016**, *13*, 405.